Hydraulic Subsurface Pump Numerical Study

G. Jax, C. Langbauer, P. Vita
Chair of Petroleum and Geothermal Energy Recovery, Chair of Drilling and Completion Engineering, Montanuniversität Leoben

Abstract

Conventional artificial lift systems are limited in their application by depth, borehole trajectory, and chemistry of the produced media. This paper presents a new hydraulic pumping system to overcome these limitations and to assure a cost-effective production in harsh environments and low gravity oil reservoirs.

The pumping system consists of a specially designed pump & piston combination, which is driven by a hydraulic pressure unit from the surface without any mechanical connection. This new pump type is designed, manufactured, and tested at the Montanuniversität Leoben, Austria. To speed up the design process the pumping concept of the hydraulic subsurface pump was validated using the open-source software toolbox OpenFOAM®.

The used transient incompressible solver *pimpleDyMFoam* allowed to tackle the challenging task of coupling a dynamic mesh movement with the fluid flow in the well. The dynamic mesh contains a sliding mesh interface between the tubing and the moving pump assembly utilizing OpenFOAM's Arbitrary Coupled Mesh Interface (ACMI), and a deforming mesh region that models the work chamber volumetric change as the piston moves up and down. The complex mesh movement is driven by fluid pressure forces acting within the pump. The acting forces are evaluated every time step and the analytically calculated mesh displacement is then imposed on the dynamic mesh in the next time step. The k-ω Shear Stress Transport turbulence model is used to resolve the turbulent flow at lower Reynolds numbers.

The conducted study provides an insight into the influence of the differential pressure, the piston geometry and its weight, as well as the well geometry on the pump’s dynamic behavior. The results are used in the optimization and further development of the hydraulic subsurface pump concept. The simulation has provided insight into this promising pumping system.

Introduction

The daily average oil consumption will reach 100 million barrels per day in the next years. To meet the growing demand huge efforts for exploring and developing new oil and gas reservoirs have to be taken by oil companies. In addition, a major emphasis is on the effective production from mature fields under economic conditions. New technologies have to be applied for recovering hydrocarbon from their reservoirs in a cost-effective manner in the future. During the production of oil from a reservoir, reservoir parameters alter and fluid properties change – in general, the oil gets heavier and the viscosity increases. At a certain point, standard recovery methods to produce oil have reached their limits, and enhanced oil recovery (EOR) methods have to be applied to continue production. Tertiary oil recovery methods include [1] three EOR techniques:

DGMK-Tagungsbericht 2018-1, ISBN 978-3-941721-86-9

- Thermal Oil Recovery

  Improving the ability of the high viscous oil to flow through the porous rock into the production well be reducing the viscosity of the oil in the reservoir by, for instance, injecting steam into the reservoir. Challenging are high temperatures, increase in water cut and especially for artificial lift systems the fact that often deviated wellbores are used to produce the oil.

- Gas Injection

  Natural gas, nitrogen, or carbon dioxide are injected to maintain the reservoir pressure high and to provide by its expansion addition oil to the producer, thus improving the displacement process. Some gases interact with the oil and reduce its viscosity. The installed completion has to be able to handle huge amounts of gas and acids that can be created when a special type of gas is injected.

- Chemical Injection

  Surface tension reducing emulsions are injected to increase the mobility of the oil. The injected chemicals, when being produced again may interact with the completion, causing an increased rate of metal loss.

The share of the individual types of tertiary recovery methods is not equally distributed on the globe. More than 100 projects worldwide employ thermal recovery and gas injection methods, whereas chemical injection projects are rarely realized. EOR wells require some kind of artificial lift system. Not all standard pumping systems match the requirements of EOR wells. Especially temperature resistance, the ability for lifting high viscous oil and working in corrosive environments, as well as the application in deviated wells and fast pump exchange are significant.

Liquid loading of gas wells becomes a significant issue in the late stage of gas production. The production rate is reduced as a result of the rising water level in the wellbore. The effective removal of the gas is necessary to ensure production. Several technologies are available, as soap sticks, capillary strings, surfactants, artificial lift system, etc. Challenges like trajectory must be met by the applied technology.

A study [2] has shown that hydraulic pumping systems and gas lift systems are favorable kinds of artificial lift systems, whereas the application of sucker rod pumps and electric submersible pumps is limited. Existing hydraulic piston pumping systems still have some limitations:

- The pump piston’s up- and downward motion is controlled by downhole components.

- Two parallel tubing strings, a called dual completion, have to be installed. The annulus is used for producing free gas, one tubing for the power fluid and the other one for the production fluid. This type of completion requires a large wellbore.

Concentric Tubular Completion

This paper presents the advantage of a concentric tubular pumping system used for a new type of hydraulic pump to recover oil and gas form that is able to overcome the above-stated limitations. Standard completions with more than one tubing string, require a lot of space and large wellbore diameters. The concentric tubular completion uses a pipe in the pipe system. This system provides three flow paths: tubing, annulus tubing–tubing and annulus casing–tubing.

Figure 1 presents the capabilities of a concentric tubular pumping system. The standard dual completion consists of an 8 5/8” casing and two 2 7/8” tubing strings. For the concentric tubular completion, the inner tubing string is a 2 7/8” pipe. The second pipe string consists of 5” pipes. The outer pipe is a 7” casing. The concentric tubular pumping system is a space-optimized system providing advantages like inter tubing – outer tubing annular cross-section is bigger than the 2 7/8” tubing inner cross-section, resulting in beneficial lower flow velocities of the lifted fluid. Smaller wellbores can be equipped with a concentric tubular completion; respectively the wellbores can be designed with smaller production casings, saving drilling costs, casing costs and time.

Standard Dual Completion	Concentric Tubular Completion

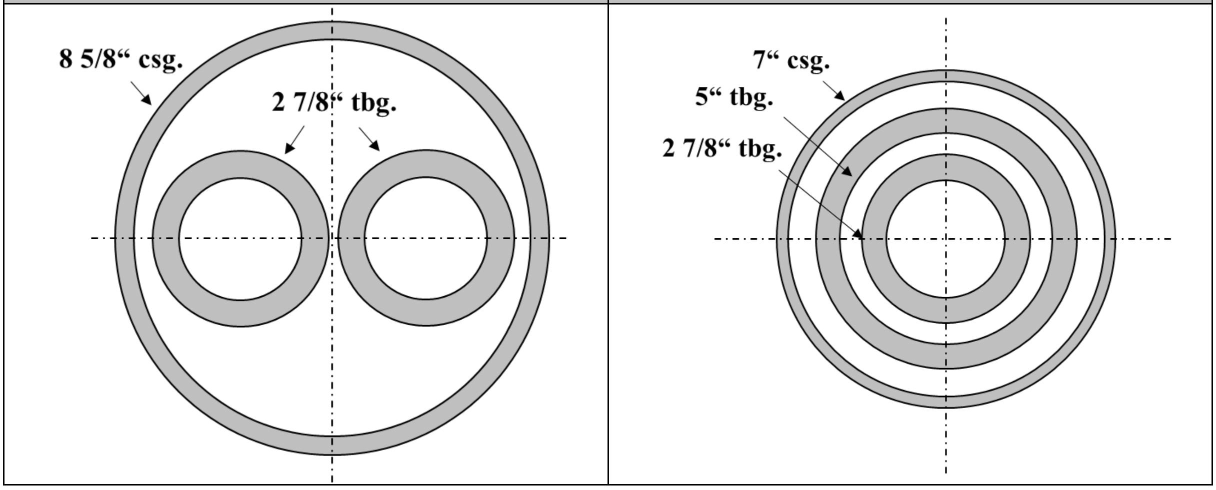

Figure 1: Comparison cross-sections (standard dual completion and concentric tubular system)

Advancements in Hydraulic Pumping Technology

The presented new hydraulic pumping system is combined with the concentric tubular completion to take advantage of its benefits. Ball valve 1 and its valve seat seals the outer tubing string and prevents mixing of the workover fluid with the reservoir fluid during system installation, thus protecting the reservoir. At the lower end of the inner tubing, a barrel and ball valve 2 are attached, to prevent undesired communication. The lower barrel is connected by a crossover to the upper one, which is slightly bigger in diameter. In the barrels, a reciprocating piston, consisting out of two plungers and a connection rod, is installed. The plunger at the bottom is of smaller size than the plunger at the top side of the piston. Ball valve 3 is at the bottom of the piston, whereas its upper end is closed. The stroke length can reach, depending on the equipment several meters. The lower piston also comprises a connection channel, connecting the intake chamber with the discharge chamber. The discharge chamber is opened by the predrilled section to the outer tubing, inner tubing annulus, and the surface. The inner tubing is filled with a hydraulic power fluid, like diesel oil or gasoline.

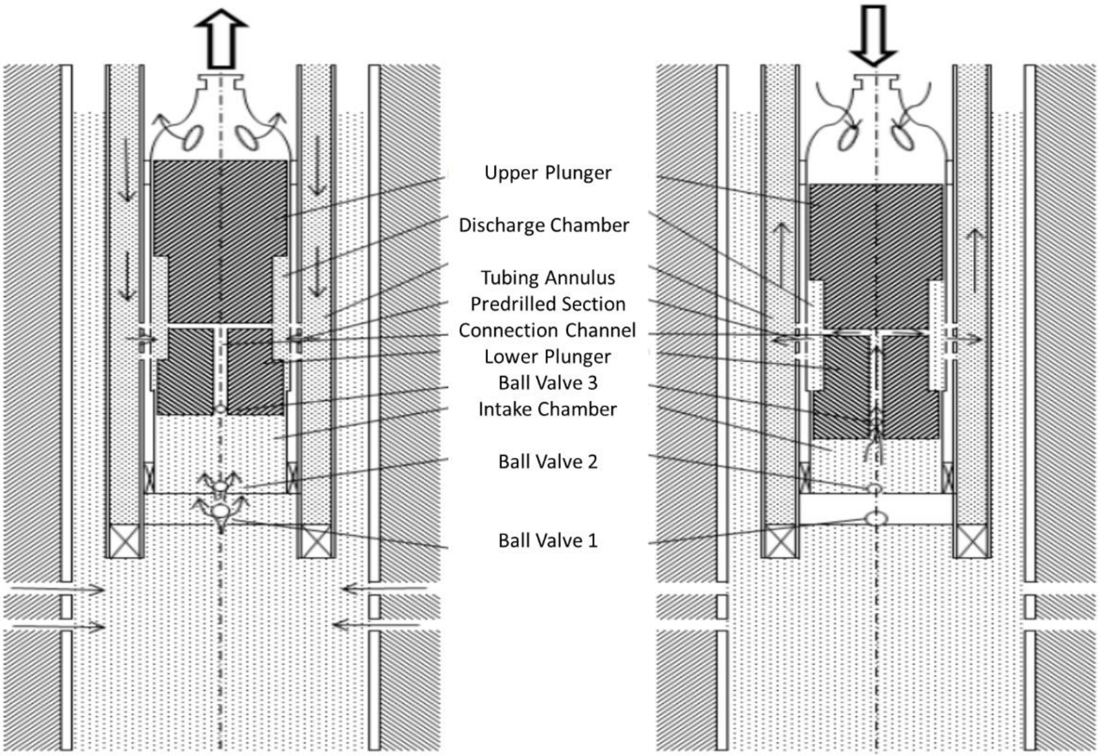

Figure 2: Hydraulic pumping system schematic drawing [3]

Working Principle

The inner tubing is at the surface connected via an automated control valve to a high-pressure vessel, filled with pressurized power fluid required during the downstroke and a low-pressure vessel for accumulating the oil during the upstroke of the downhole hydraulic pump. The pressure vessels are connected by a hydraulic pump. The outer tubing – inner tubing annulus is connected to the gathering system, having a constant pressure. The intake chamber is connected to the reservoir by ball valve 1. To move the reciprocating piston assembly downward, which represents the pumping stroke, the pressure of the power fluid at the inner tubing is increased by connecting it to the high-pressure vessel. At this moment the traveling valve (ball valve 3) opens, while ball valve 2 and ball valve 3 close and the fluid from the intake can flow through the connection channel into the discharge chamber an into the tubing annulus. At the lower dead center, it is possible by using a check valve to inject inhibiting power fluid into the produced fluid, to prevent corrosion of the tubing string and to reduce friction pressure losses by thinning of the fluid. To move the reciprocating piston assembly upward the pressure of the hydraulic power fluid in the inner tubing is reduced by connecting it to the low-pressure vessel. Ball valve 3 is closed, but ball valve 1 and 2 are opened to allow filling of the intake chamber with reservoir fluid. The pressure of the produced fluid at the discharge pushes the plunger assembly upward.

To investigate the performance of the new hydraulic pumping system, tests at the Pump Testing Facility at the Montanuniversität Leoben and numerical simulations have been performed. The pump design incorporates existing, standardized equipment and some additional modified components. The pump tested, consists out of a 275/225 plunger, having a stroke length of 1.2 meters.

Numerical Simulation

The concept of the hydraulic subsurface pump was validated using Computational Fluid Dynamics (CFD). A simplified 2D pump model was developed and implemented using the open-source software toolbox OpenFOAM [4] and its supporting library swak4Foam [5].

Fluid Flow Model

The produced fluid is assumed incompressible. Thus transient incompressible Navier-Stokes equations are governing the fluid flow during the pump cycle:

$$\nabla.\boldsymbol{u} = 0 \qquad \text{(Eq.1a)}$$

$$\frac{\partial \boldsymbol{u}}{\partial t} + \nabla.(\boldsymbol{u}\boldsymbol{u}) = -\nabla P + \nabla.\{(\nu + \nu_{\mathrm{t}})[(\nabla \boldsymbol{u} + (\nabla \boldsymbol{u})^{\mathrm{T}}]\} \qquad \text{(Eq.1b)}$$

where $\boldsymbol{u}$ represents the fluid velocity [$m.s^{-1}$], P is the kinematic pressure [$m^2.s^{-2}$], v and v_t are kinematic viscosity [$m^2.s^{-1}$] and kinematic turbulent viscosity [$m^2.s^{-1}$] respectively, and t denotes time [s].

Both equations, continuity (Eq.1a) and momentum (Eq.1b), are disconnected from the energy equation due to the constant density ρ [$kg.m^{-3}$], what simplifies the modeling as the thermodynamic state of the system can be neglected.

The turbulent viscosity v_t is supplied by the turbulence model. The selected turbulence model is the two-equation *k-ω* Shear-Stress Transport (SST) by F. R. Menter [6] for Reynolds averaged simulation (RAS). The *k-ω* SST model is a low-Re turbulence model and can describe laminar to turbulent flow transition within the pump.

The discretization of the equation system [7] and its implementation is realized by OpenFOAM's solver *pimpleDyMFoam*. The solver *pimpleDyMFoam* supports the dynamic mesh movement [8, 9] needed to model the reciprocating piston and the intake chamber in the simulation.

Computational Grid

The simplified 2D model of the pump was created using OpenFOAM's utility *blockMesh*. The resulting parameterized computational grid, see Figure 3, is a 2D multi-block orthogonal tetrahedral mesh with ~34.000 tetrahedral cells.

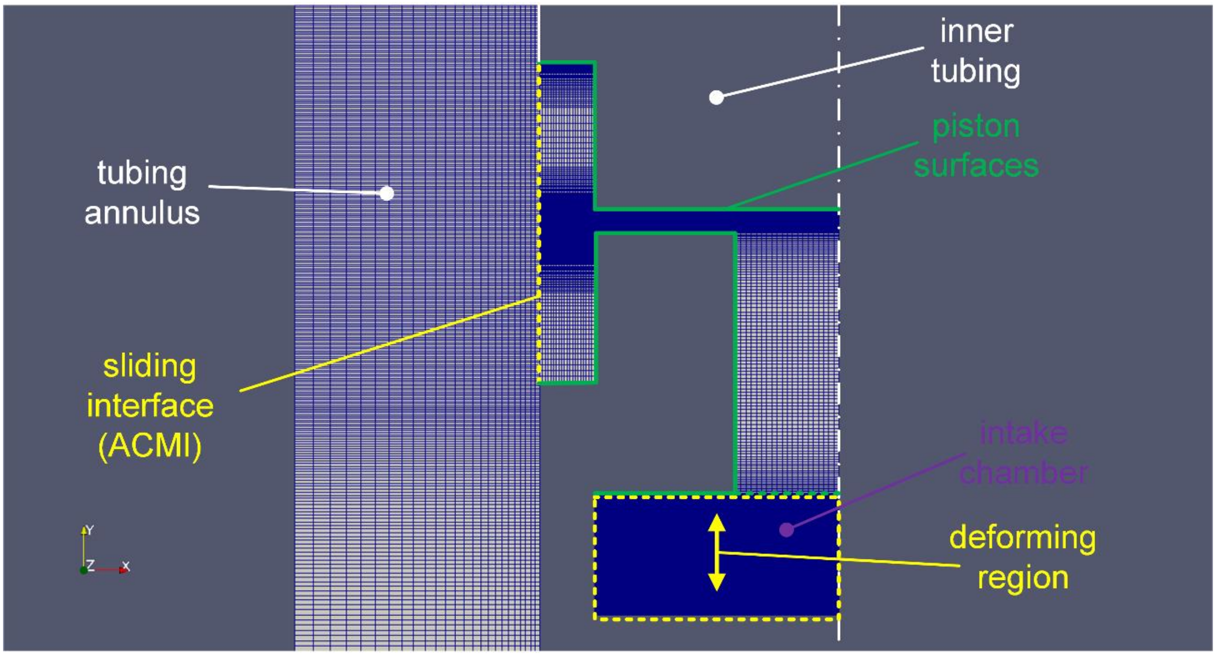

Figure 3: Computational grid detail (x-axis scaled 30×)

The mesh incorporates advanced features such as Arbitrary Coupled Mesh Interface (ACMI) to model the piston sliding along the tubing annulus and deforming mesh region modeling the intake chamber volumetric change.

Pump Cycle

The pump cycle is governed by forces, acting on the reciprocating piston inside the pump, see Figure 4. The hydrostatic pressure forces acting on the pump in the static equilibrium are balanced and thus omitted.

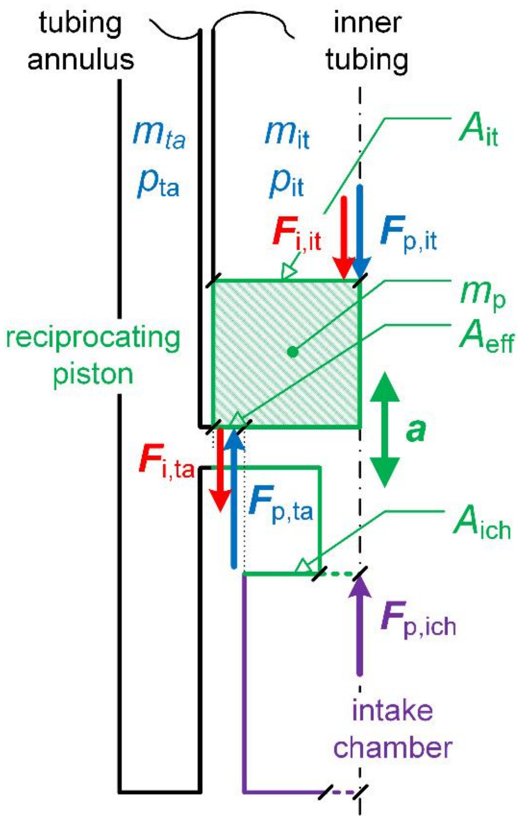

Figure 4: Forces acting on the piston

The pump cycle is controlled by the manipulation of the inner tubing pressure p_{it} [Pa] acting on the reciprocating piston through the power fluid. The resulting pressure force $F_{p,it}$ [N]:

$$F_{\mathrm{p,it}} = p_{\mathrm{it}} A_{\mathrm{it}}, \qquad \text{(Eq.2)}$$

where A_{it} is the piston area [m^2] in the inner tubing, is balanced against the pressure force $F_{p,ta}$ in the tubing annulus acting on the effective cross-section area A_{eff} [m^2]:

$$F_{\mathrm{p,ta}} = p_{\mathrm{ta}} A_{\mathrm{eff}} = p_{\mathrm{ta}}(A_{\mathrm{it}} - A_{\mathrm{ich}}), \qquad \text{(Eq.2)}$$

where p_{ta} is the tubing annulus pressure [Pa] and A_{ich} is the piston area [m^2] inside the intake chamber, and the pressure force $F_{p,ich}$ [N] in the intake chamber:

$$F_{\mathrm{p,ich}} = p_{\mathrm{ich}} A_{\mathrm{ich}}, \qquad \text{(Eq.3)}$$

where p_{ich} is the pressure [Pa] acting on the piston in the intake chamber, and A_{ich} represents the piston area [m^2] in the intake chamber. The intake chamber pressure p_{ich} acting on the piston is supplied by the numerical simulation.

The inner tubing pressure is a function of time $p_{it}(t)$ and allows analysis of the various pump cycles based on the supplied inner tubing pressure profile, see Figure 5, where p_{eq} is the equilibrium pressure [Pa] when the piston is static, and Δp_{op} is the operative pressure difference [Pa].

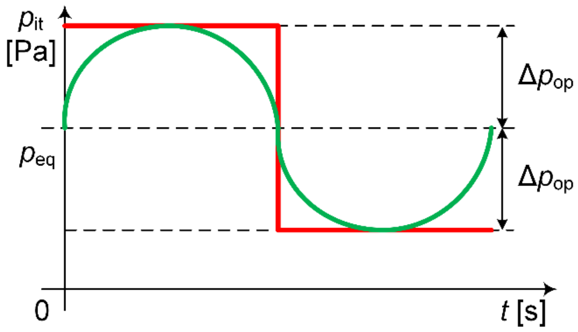

Figure 5: Inner tubing pressure profiles

The total pressure difference will initiate the movement of the reciprocating piston, leading to upstroke or downstroke. Once the piston starts to move, additional inertial forces start to act on the piston.

The most prominent is the power fluid inertial force $F_{i,it}$ [N] within the inner tubing acting against the piston:

$$F_{\mathrm{i,it}} = m_{\mathrm{it}} a \tag{Eq.4}$$

where m_{it} is the mass of the power fluid [kg] above the piston, and a is the piston acceleration [m.s^{-2}].

The counterpart of the power fluid inertial force $F_{i,it}$ is the production fluid inertial force $F_{i,ta}$ [N] referencing the tubing annulus:

$$F_{\mathrm{i,ta}} = m_{\mathrm{ta}} c_{a,\mathrm{ta}} a \tag{Eq.5}$$

where the m_{ta} is the mass of the production fluid [kg] in the tubing annulus and $c_{a,ta}$ is the inertia coefficient for the tubing annulus acceleration [-].

The resulting piston acceleration a [m.s^{-2}] is then defined as:

$$a = \frac{\sum_k F_k}{\sum_l m_l} = \frac{\left(F_{\mathrm{p,ta}} + F_{\mathrm{p,ich}} - F_{\mathrm{p,it}}\right)}{\left[m_{\mathrm{p}} + m_{\mathrm{it}} + (c_{a,\mathrm{ta}} m_{\mathrm{ta}})\right]} \tag{Eq.6}$$

where m_p is the piston mass [kg].

As the acceleration is considered uniform per time step Δt [s], we can directly calculate the piston velocity v [m.s^{-1}] and displacement s [m]:

$$v = v_0 + a\Delta t \tag{Eq.7}$$

$$s = s_0 + v_0 \Delta t + \frac{1}{2} a \Delta t^2 \tag{Eq.8}$$

where v_0 and s_0 represent the piston velocity [m.s^{-1}] and displacement [m] from the previous time step respectively.

The resulting piston displacement s is introduced into the simulation in the form of the algebraic expressions that prescribe the mesh movement. The mesh points are recalculated each time step by the OpenFOAM's *displacementLayeredMotion* solver to account for the change of the piston position and the volumetric change of the intake chamber.

The mesh movement influences the fluid flow within the pump. The no-slip velocity boundary conditions at the piston walls reflect the piston velocity and thus drive the fluid flow.

Results

The following scenario was defined for the numerical investigation:

Pump setting depth:	1000 m		
Produced fluid (water):	1000 kg.m^{-3}	Power fluid (gasoline):	750 kg.m^{-3}
Reservoir pressure:	3.7 MPa (37 bar)	Flow line pressure:	5 MPa (50 bar)

Running the simulation for the upstroke leads to the pressure and velocity fields shown in Figure 6 and Figure 7 for first 2 seconds of simulated time. The pump assembly accelerates as expected to result in a rapid increase of the covered distance, see Figure 8, changing the geometry of the intake chamber in the process.

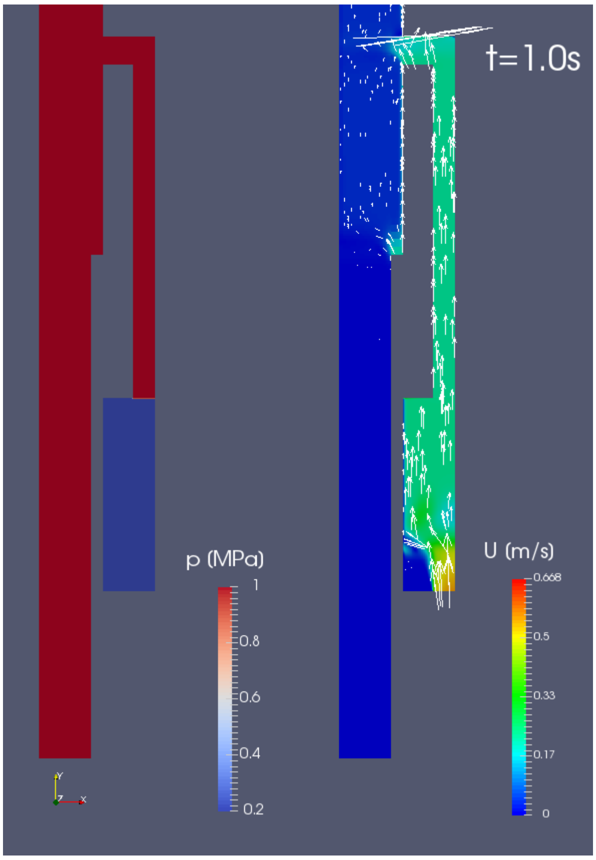

Figure 6: Upstroke, t=1s (x-axis scaled 5×)

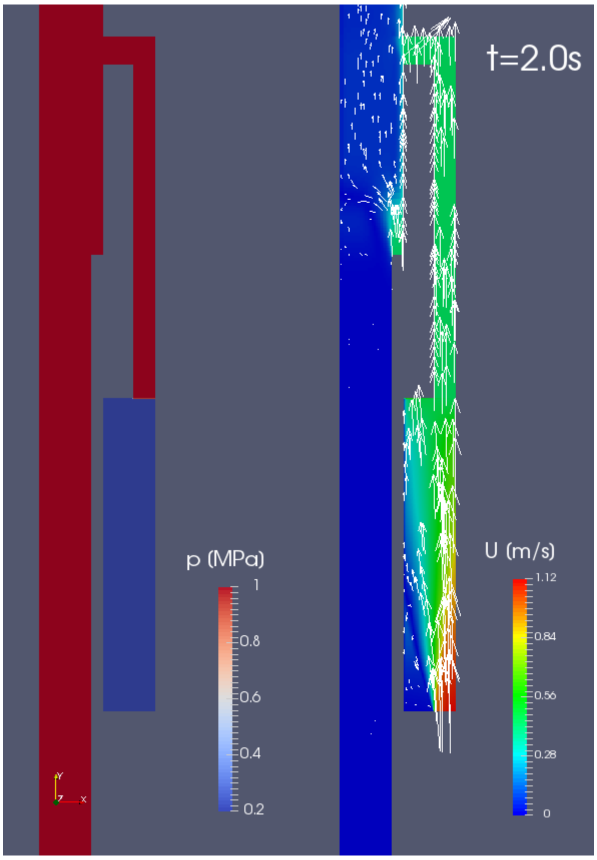

Figure 7: Upstroke, t=2s (x-axis scaled 5×)

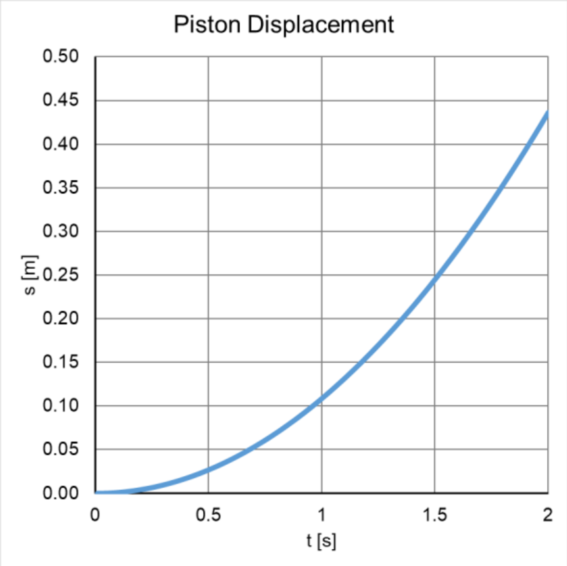

Figure 8: Upstroke (piston displacement)

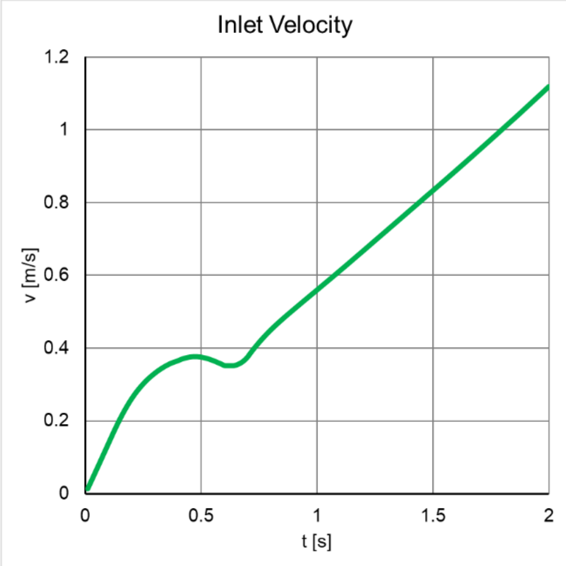

Figure 9: Upstroke (inlet velocity at the intake chamber)

An interesting behavior of the inlet velocity at the pump intake was observed, see Figure 9, which is the result of the pressure dynamics inside the intake chamber.

Conclusion and Outlook

The concentric tubular pumping system allows the easy inject inhibited power oil into the production annulus and venting of free gas to surface. The new hydraulic pump provides advantages like no mechanical connection to the surface, no over- and under-traveling of the plunger assembly and the applicability to any kind of inclined wellbore.

The numerical study of the hydraulic subsurface pump delivers an insight into the pump system behavior. Due to that, it is possible to analyze the pump dynamics for different operation modes and to investigate connected effects. The simulation will be further optimized for the advancement of this new hydraulic pump.

References

[1] US Department of Energy, "Enhanced Oil Recovery," (2018)

[2] C. Langbauer, et al., „Hydraulic Concentric Tubular Pumping System for lifting Oil in EOR Completions," SPE-190344-MS, Muscat, Oman, (2018)

[3] H. Hofstätter, "Pump system," Patent number WO2011069517 A1 (2009)

[4] The OpenFOAM Foundation, OpenFOAM. http://openfoam.org/ (2017)

[5] B. F. W. Gschaider, swak4Foam Library (2017)

[6] F. R. Menter, "Two-equation eddy-viscosity turbulence models for engineering applications," AIAA Journal, vol. 32, no. 8, pp. 1598–1605 (1994)

[7] H. Jasak, "Error Analysis and Estimation for the Finite Volume Method with Applications to Fluid Flows," Ph.D. Thesis, Department of Mechanical Engineering, Imperial College of Science, Technology and Medicine, London (1996)

[8] H. Jasak, "Dynamic Mesh Handling in OpenFOAM," in 47th AIAA Aerospace Sciences

Meeting including the New Horizons Forum and Aerospace Exposition, Orlando, Florida, USA (2009)

[9] H. Jasak and Z. Tukovic, “Automatic mesh motion for unstructured finite volume method,” Transactions of FAMENA, vol. 30, pp. 1–18 (2007)